LETTERS

Potentiation of cortical inhibition by visual deprivation

Arianna Maffei[1], Kiran Nataraj[1], Sacha B. Nelson[1] & Gina G. Turrigiano[1]

The fine-tuning of circuits in sensory cortex requires sensory experience during an early critical period. Visual deprivation during the critical period has catastrophic effects on visual function, including loss of visual responsiveness to the deprived eye[1–3], reduced visual acuity[4], and loss of tuning to many stimulus characteristics[2,5]. These changes occur faster than the remodelling of thalamocortical axons[6], but the intracortical plasticity mechanisms that underlie them are incompletely understood. Long-term depression of excitatory intracortical synapses has been proposed as a general candidate mechanism for the loss of cortical responsiveness after visual deprivation[7,8]. Alternatively (or in addition), the decreased ability of the deprived eye to activate cortical neurons could be due to enhanced intracortical inhibition[9,10]. Here we show that visual deprivation leaves excitatory connections in layer 4 (the primary input layer to cortex) unaffected, but markedly potentiates inhibitory feedback between fast-spiking basket cells (FS cells) and star pyramidal neurons (star pyramids). Further, a previously undescribed form of long-term potentiation of inhibition (LTPi) could be induced at synapses from FS cells to star pyramids, and was occluded by previous visual deprivation. These data suggest that potentiation of inhibition is a major cellular mechanism underlying the deprivation-induced degradation of visual function, and that this form of LTPi is important in fine-tuning cortical circuitry in response to visual experience.

In many animals, including rodents and primates, visual deprivation during a critical period induces a permanent loss of visual responsiveness and acuity referred to as amblyopia[11,12]. In rodents, monocular deprivation during this critical period induces a rapid (within two days) loss of responsiveness to the deprived eye, followed more slowly (longer than five days) by increased responsiveness to the spared eye, indicating that these are separable processes that probably occur by distinct mechanisms[3]. Little is known about the synaptic changes that underlie the loss of responsiveness to the deprived eye. Here we used whole-cell recordings in rat visual cortical slices[13] to selectively examine changes in excitatory and inhibitory microcircuitry within layer 4 after the suturing of one eyelid. In rodents, about two-thirds of the visual cortex is driven exclusively by the contralateral eye (monocular cortex), whereas a small binocular zone also receives a weak ipsilateral projection; most visual function is thus mediated solely by inputs from one eye. Visual deprivation (VD)-induced loss of cortical responsiveness and reduced visual acuity do not depend on competitive interactions between the two eyes[4,11], so the underlying mechanism can be studied in monocular cortex. Because in binocular cortex the synapses driven by the two eyes are intermingled, we restricted our analysis to monocular cortex, where we could probe the mechanisms underlying loss of responsiveness to the deprived eye by analysing connections that were unambiguously affected by the deprivation, and without contamination from the slower potentiation of inputs from the non-deprived eye[3].

To determine whether VD depresses excitatory synapses within layer 4, we examined monosynaptic connections between star pyramids, the major class of excitatory neuron within layer 4 of V1. VD between postnatal day 18 (P18) and P21 had no effect on excitatory postsynaptic current (EPSC) amplitude (Fig. 1a–c; control, $n = 73$; deprived, $n = 59$; $P = 0.57$), the probability of finding connected pairs (control, 10.7% of 739 tested; deprived, 11.4% of 553 tested), or on short-term plasticity (Fig. 1b; probed with trains of five spikes at 20 Hz, steady-state depression 42.3 ± 4.5% for control and 43.7 ± 3.3% for deprived; $P = 0.78$). Additionally, spike-timing-dependent long-term depression (LTD)[14] was similar between hemispheres (Fig. 1d–f; $P = 0.43$). Taken together with our previous data showing no effect of VD on miniature EPSCs onto star pyramids at this developmental stage[15], these data indicate that two days of VD during the critical period leaves excitatory transmission and plasticity onto star pyramids in layer 4 unaltered.

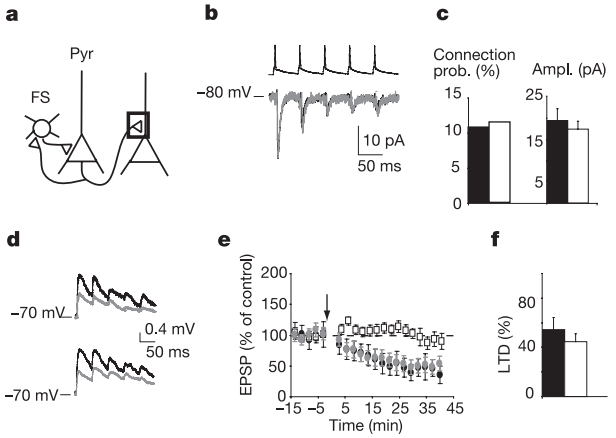

Figure 1 | VD between P18 and P21 has no effect on recurrent excitatory star pyramid connections. **a**, Diagram of excitatory star pyramid (Pyr) connections. **b**, Overlaid EPSCs from example control (black) and deprived (grey) pairs, showing presynaptic spike train (top) and postsynaptic current (bottom). **c**, Average EPSC amplitude (right) and connection probability (left) for control (filled bars) and deprived (open bars) pairs. **d**, Example LTD experiments (in current clamp) from control (top) and deprived (bottom) hemispheres (black, before pairing; grey, after pairing). **e**, Time course of EPSPs for control and deprived hemisphere pairs without LTD pairing protocol (white squares), and for control and deprived hemisphere pairs with LTD pairing protocol (black and grey circles, respectively). Arrow indicates the time of the induction protocol. **f**, Average magnitude of pairing-induced LTD for control (filled bar) and deprived (open bar) pairs. Where shown, error bars are s.e.m.

[1]Department of Biology and Center for Behavioral Genomics, Brandeis University, Waltham, Massachusetts 02454, USA.

To analyse feedback inhibitory circuitry within layer 4, we obtained paired recordings between FS cells and star pyramids to analyse star pyramid to FS-cell excitation, and FS-cell to star-pyramid inhibition (Fig. 2). We focused on this microcircuit because FS cells are a major source of inhibition within layer 4, are important in regulating network excitability during the precritical period[13] and have been implicated in the initiation of critical period plasticity[16]. FS cells receive much of their excitatory drive from star pyramids (Fig. 2a)[17]. VD induced a threefold increase in the amplitude of the star-pyramid to FS-cell EPSC (Fig. 2b, c; $P < 0.01$), accompanied by an increase in steady-state depression (control, to 42.9 ± 6.6% of initial value; deprived, to 69.2 ± 6.7%; $P < 0.006$), and no significant change in connection probability (control, 57.4% of 47 tested; deprived, 53.5% of 41 tested). Thus, excitatory synapses within layer 4 are differentially regulated by VD according to their target: whereas connections from star pyramids to star pyramids remain constant, connections from star pyramids to FS cells are markedly increased in amplitude. This should serve to increase excitatory drive to FS cells and boost inhibition within layer 4.

We next determined the effect of VD on FS-cell to star-pyramid inhibitory synapses (Fig. 2d–f; the reversal potential was −49.6 ± 1.4 mV, close to the calculated chloride reversal potential, E_{Cl}, of −50.3 mV, and the holding potential was −80 mV, so currents were inward). There was a threefold increase in inhibitory postsynaptic current (IPSC) amplitude in the deprived hemisphere (Fig. 2e, f; control $n = 22$, deprived $n = 23$; $P < 0.01$). No significant differences were observed in connection probability (control, 50.0% of 50 tested; deprived, 61.9% of 42 tested) or short-term plasticity (steady-state depression: control, 71.5 ± 4.9%; deprived, 63.5 ± 5.4%; $P = 0.17$). The measured reversal potential was not different between control and deprived connections, when measured in whole-cell configuration (control, −49.6 ± 1.4 mV; deprived, −48.5 ± 1.8 mV), or with gramicidin-perforated patch recordings (Supplementary Fig. 1; control, −89.5 ± 0.7 mV; deprived, −88.5 ± 0.7 mV; $n = 3$). Last, there was no significant change in the strength of inhibition between FS cells (Supplementary Fig. 2; control, 21.9 ± 6.3 pA, $n = 4$; deprived, 26.1 ± 9.5 pA, $n = 3$).

Our data show that VD markedly and selectively potentiates both components of the feedback inhibitory loop between star pyramids and FS cells, indicating that the balance between excitation and inhibition onto star pyramids has shifted to favour inhibition. Increased inhibition onto star pyramids should damp their activity; to test this we compared the spontaneous firing rates of star pyramids in slices derived from control and deprived cortex, as described previously[13]. We showed previously that VD during a precritical period just around eye opening (P14–P17) increases spontaneous activity of star pyramids[13]; in contrast, VD between P18 and P21 produced a more than tenfold reduction in spontaneous firing of star pyramids in the hemisphere driven by the deprived eye (Fig. 3; control, 3.34 ± 0.62 Hz, $n = 10$; deprived, 0.22 ± 0.07 Hz, $n = 10$; $P < 0.003$); a similar reduction was induced by VD between P21 and P24 (Fig. 3b). Although additional factors may contribute to this reduced excitability, a major cause is likely to be the potentiation of feedback inhibition.

Some inhibitory synapses can undergo LTPi[18–20], raising the possibility that VD increases the amplitude of FS-cell to star-pyramid connections by inducing LTP at this synapse. We used a current clamp protocol to induce LTPi reliably in the control hemisphere, by pairing FS-cell firing (trains of ten spikes at 50 Hz, repeated 20 times at 0.1 Hz) with subthreshold depolarization of the postsynaptic star pyramid (to between −60 and −55 mV; Fig. 4a, b, control). This reliably potentiated inhibitory postsynaptic potentials (IPSPs) to about 150% of baseline ($n = 9$; $P < 0.002$; all nine connections showed potentiation of more than 25%), with no changes in reversal potential (baseline, −47.6 ± 1.2 mV; induced, −48.7 ± 1.1 mV; $n = 9$; $P = 0.3$), and no change in paired-pulse depression (baseline, 35 ± 2%; induced, 32 ± 2%; $n = 9$; $P = 0.56$). Presynaptic firing alone (in the absence of postsynaptic depolarization) had no effect on IPSP amplitude (Fig. 4b, triangles); neither did postsynaptic depolarization alone (89.7 ± 7.7% of control, $n = 3$; $P = 0.37$). In addition, various combinations of presynaptic and postsynaptic firing (presynaptic 10 ms before postsynaptic at 5 or 20 Hz, presynaptic 10 ms after postsynaptic at 20 Hz, presynaptic and postsynaptic together at 50 Hz), induced no change in synaptic strength (Fig. 4c, control, $n = 12$). Thus, LTPi at this synapse requires presynaptic spiking coupled with subthreshold postsynaptic depolarization but is prevented by coincident presynaptic and postsynaptic firing.

If LTPi underlies the VD-induced potentiation of inhibition they should share the same expression mechanism(s). To examine this more closely we performed an additional set of LTPi experiments ($n = 5$) in which we measured synaptic currents before and after LTPi (induced in current clamp as above), so that we could carefully analyse short-term plasticity and the coefficient of variation (CV). Comparing the CV of FS-cell to star-pyramid synapses in the control, deprived and LTPi cases revealed that both VD and LTPi significantly

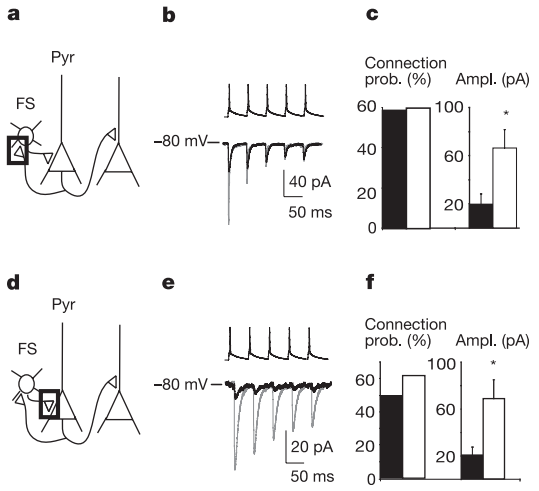

Figure 2 | VD potentiates feedback inhibition within layer 4. **a**, **b**, EPSCs from star pyramids (Pyr) onto FS neurons (**a**) were increased in amplitude by VD. **b**, Overlaid EPSCs from example control (black) and deprived (grey) pairs. **c**, Average connection probability and EPSC amplitude for control (filled bars) and deprived (open bars) pairs. **d**, **e**, IPSCs from FS cells onto star pyramids (**d**) were increased in amplitude by VD. **e**, Overlaid IPSCs from example control (black) and deprived (grey) pairs. **f**, Average connection probability (left) and IPSC amplitude (right) for control (filled bars) and deprived (open bars) pairs. Asterisk indicates statistical significance. Where shown, error bars are s.e.m.

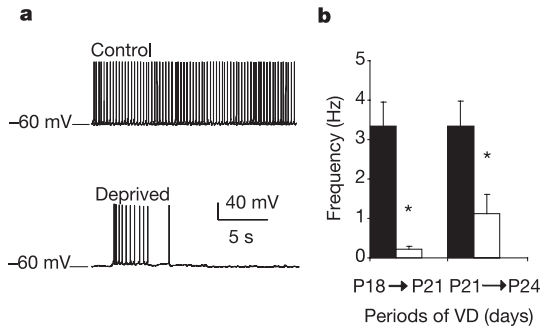

Figure 3 | VD suppresses spontaneous firing of star pyramids. **a**, Example recordings from star pyramids in slices derived from the control or deprived hemisphere, after VD between P18 and P21. **b**, Average firing rates for control (filled bars) and deprived (open bars) star pyramids after 2 days of VD during the ages indicated. Asterisk indicates statistical significance. Where shown, error bars are s.e.m.

reduced the CV (Fig. 4d, CV) but did not affect the paired-pulse ratio (Fig. 4d, PP ratio). To examine a possible postsynaptic contribution we performed non-stationary peak-scaled fluctuation analysis on the IPSCs (Supplementary Fig. 3). This revealed no difference in single-channel conductance between conditions (Fig. 4d, γ) but a significant increase in open channel number, as predicted if quantal content goes up; for both VD-induced potentiation and LTPi the increase in the number of open channels could fully account for the increase in current (Fig. 4e, f). Thus both forms of plasticity share the same expression characteristics.

A standard way of relating *in vitro* to *in vivo* plasticity phenomena is to ask whether the latter occludes the former: if VD increases inhibitory transmission through LTPi, further induction of LTPi should be occluded. To test for such occlusion we compared LTPi in the control and deprived hemispheres. The same protocol that induced LTPi in the control hemisphere (Fig. 4a, b, control) did not induce LTP in the deprived hemisphere; rather, it induced a robust LTD (Fig. 4a, b, deprived, $n = 8$; $P < 0.01$) with no change in the reversal potential (control, -48.9 ± 0.9 mV; induced, -49.3 ± 0.8 mV; $n = 8$; $P = 0.7$) or paired-pulse depression. The induction protocols that were ineffective at inducing inhibitory plasticity in the control hemisphere were also ineffective in the deprived hemisphere (Fig. 4c, deprived, $n = 12$), indicating that the induction requirements might have been unaffected by VD. These data suggest that VD potentiates FS-cell to star-pyramid synapses through an LTPi-like process, which saturates LTPi and unmasks a competing LTD. Consistent with this was our observation that a second induction in the control hemisphere depressed synaptic transmission back to control levels, whereas in the deprived hemisphere it induced further LTD (Supplementary Fig. 4).

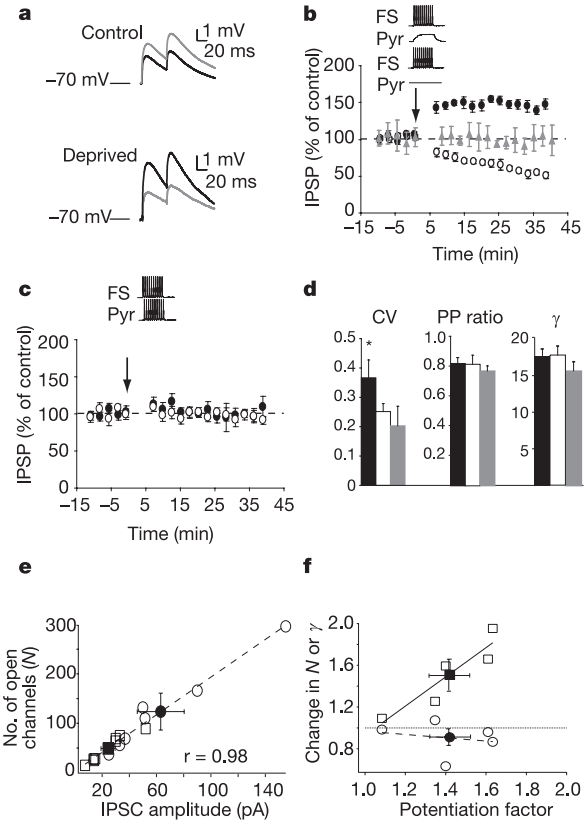

Figure 4 | Inhibitory LTP at FS-cell to star-pyramid synapses is occluded by previous VD. a, **b**, Pairing FS-cell firing with subthreshold star pyramid depolarization produced LTPi in the control hemisphere but LTDi in the deprived hemisphere. **a**, Top: example IPSPs from the control hemisphere before (black) and after (grey) pairing. Bottom: example IPSCs from the deprived hemisphere before pairing (black) and after pairing (grey). **b**, Average time course of IPSCs after pairing of FS cell firing with subthreshold star pyramid depolarization (inset, top) for control (filled circles) or deprived (open circles) connections. FS cell firing alone (inset, bottom) had no effect on IPSC amplitude (grey triangles). Arrows in **b** and **c** indicate time of the induction protocol. **c**, No plasticity was induced when star pyramid and FS cells were fired together. Filled circles, control pairs; open circles, deprived pairs. **d**, Bar plot showing CV, PP ratio and γ for control (black bars), deprived (white bars) and after LTPi induction (grey bars). Asterisk indicates statistical significance. **e**, Correlation between number of open channels (N) and IPSC amplitude for control (squares) and deprived (circles) pairs; each open symbol represents one pair; average values are represented by the filled symbols. The dashed line indicates the best linear fit ($r = 0.98$). **f**, Correlation between changes in N (open squares) or γ (open circles) and the potentiation factor (LTP amplitude divided by baseline amplitude) for each pair that underwent LTPi induction. Filled square, average N versus LTP factor; filled circle, average γ versus LTP factor. The solid line shows the best linear fit of N versus LTP factor ($r = 0.92$); the dashed line shows the best fit to γ versus LTP factor ($r = -0.2$). Where shown, error bars are s.e.m.

We have shown that a major effect of visual deprivation is a marked potentiation of feedback inhibition within layer 4 (see diagram, Supplementary Fig. 5). Our data support the idea that this occurs through an LTPi-like process that requires presynaptic firing coupled with subthreshold postsynaptic depolarization but is prevented by correlated presynaptic and postsynaptic firing. Because of these novel induction characteristics[18–20], LTPi at this synapse should only be induced when presynaptic and postsynaptic firing occur independently. Eye closure might produce just such an activity mismatch, because a decrease in the activity of star pyramids after eye closure should increase the probability that FS cells (which have a higher spontaneous firing rate[21,22]) will fire in the absence of postsynaptic star pyramid firing. FS cells mediate inhibition that spreads mainly horizontally within a cortical layer[23], and are extensively electrically coupled[24]. These properties allow them to inhibit a large population of excitatory neurons simultaneously. Increased feedback inhibition between FS cells and star pyramids should decrease the gain of incoming visual input by limiting the intracortical propagation and amplification of sensory information. As well as shaping cortical response properties, the inhibition of FS cells is important in initiating the critical period[16], raising the possibility that inhibitory potentiation could be a necessary trigger for additional plasticity mechanisms such as those underlying the slower increase in responsiveness to the non-deprived eye[3].

Some form of lateral, surround, or opponent inhibition is crucial for the function of many diverse microcircuits[25–28]. In addition to contributing to the pathological changes in cortical function that follow sensory deprivation, the novel form of LTPi described here could serve as a general mechanism for sharpening lateral or opponent inhibition, because LTPi will strengthen inhibition onto neurons that are driven less effectively than the presynaptic interneuron by the same sensory stimuli. Finally, the ability of inhibitory plasticity to change sign as a function of previous history indicates that FS inhibition might be dynamically expanded or retracted by particular patterns of sensory input.

METHODS

General methods. Methods and solutions were as reported previously[13]. Monocular eyelid suture was performed late on P18 and animals were killed for recording early in P21; for some experiments (where indicated in the text) sutures were performed between P21 and P24. Coronal slices containing primary visual cortex were prepared from deprived and control hemispheres, and visualized patch clamp recordings were obtained from layer IV in the monocular region of V1. Neurons were filled with biocytin for post hoc reconstruction and were classified as described previously on the basis of morphology, firing properties, and synaptic properties[13]. Neurons were included if resting potentials were < -60 mV, input resistances were > 80 MΩ, series resistances were < 15 MΩ, and these parameters did not change more than 10% during the recording. Solutions were as described previously[13].

Perforated patch recordings. Perforated patch recordings of star pyramids with

the use of gramicidin D were used to compare the $GABA_A$ reversal potential between control and deprived hemispheres. Perforated patch internal solution had the following composition (in mM): KCl 130, EGTA 5, $CaCl_2$ 0.5, $MgCl_2$ 2, HEPES 10; pH made to 7.35 with KOH. Gramicidin D (50 $\mu g\,ml^{-1}$) was added to the internal solution before recordings and was sonicated for at least 30 s. The artificial cerebrospinal fluid for perforated patch recording contained DL-2-amino-5-phosphonopentanoic acid (50 μM) and 6,7-dinitroquinoxaline-2,3(1H,4H)-dione (20 μM). IPSCs were obtained by extracellular stimulation with a tungsten bipolar electrode (Harvard apparatus) positioned 40–100 μm from the recording site. The stimulation intensity was adjusted for each recording to the minimum needed to avoid failures. The equilibrium potential was obtained by measuring the voltage at the intersection between the holding-current and synaptic-current *I–V* curves as described in ref. 29 (Supplementary Fig. 1).

Plasticity induction protocols. Plasticity experiments were performed in current clamp to assess the role of presynaptic and postsynaptic firing in plasticity induction. A small bias current was injected into both presynaptic and postsynaptic neurons to keep their membrane potentials close to −70 mV between current injections. For LTD at recurrent star pyramid synapses, baseline synaptic transmission properties were assessed with trains of five presynaptic action potentials at 20 Hz, repeated at 0.05 Hz. During induction, presynaptic action potentials were paired, with a 10-ms delay, with postsynaptic action potentials (ten pairings at 0.1 Hz) as described[14]. For FS-cell to star-pyramid connections, baseline synaptic transmission properties were assessed with two presynaptic action potentials at 20 Hz, repeated at a frequency of 0.05 Hz. LTPi was successfully induced by pairing ten presynaptic action potentials at 50 Hz with postsynaptic depolarization to between −60 and −55 mV (20 pairings at 0.1 Hz). The protocols that failed to induce LTPi were as follows: 10-ms presynaptic before postsynaptic (control $n = 3$; deprived $n = 3$) or postsynaptic before presynaptic (control $n = 3$; deprived $n = 3$) pairing at 20 Hz (20 repetitions at 0.1 Hz); 10 ms presynaptic before postsynaptic pairing at 5 Hz for 30 s (ref. 19) (control $n = 3$, deprived $n = 3$); and presynaptic and postsynaptic firing together at 50 Hz (20 repetitions at 0.1 Hz; control $n = 3$; deprived $n = 3$). To perform noise analysis on IPSCs before and after LTPi induction, synaptic currents were recorded in voltage clamp; after a 10-min baseline, recordings were switched into current clamp for LTPi induction (pairing presynaptic firing at 50 Hz with postsynaptic depolarization to −60 mV as above); recordings were then switched back to voltage clamp to measure LTP of synaptic currents.

Non-stationary peak-scaled fluctuation analysis (NPSNA). NPSNA was performed using standard methods as described previously[30]. In brief, for each unitary connection the average evoked IPSC was scaled to the peak of each individual IPSC and subtracted; the variance about the mean was then computed during the decay phase of the IPSCs (in 100-μs bins) and plotted against the mean current (Supplementary Fig. 3). The resulting relationship was well fitted with a parabolic equation from which could be extracted estimates of the single-channel conductance (γ) and the number of open channels (N). For LTPi experiments, this procedure was repeated for baseline currents and for post-induction currents.

Statistical tests. All data are expressed as mean ± s.e.m. for the number of pairs (or neurons) indicated. Statistical significance was determined by using two-tailed unpaired *t*-tests, except as follows. To determine the statistical significance of LTP and LTD within a condition, paired *t*-tests were performed on baseline amplitudes versus amplitudes 30 min after potentiation. The significance of changes in connection probability was tested with a χ^2 for contingency test.

Received 22 April; accepted 14 July 2006.
Published online 23 August 2006.

1. Wiesel, T. N. & Hubel, D. H. Single cell responses in striate cortex of kittens deprived of vision in one eye. *J. Neurophysiol.* **26,** 1003–1017 (1963).
2. Fagiolini, M., Pizzorusso, T., Berardi, N., Domenici, L. & Maffei, L. Functional postnatal development of the rat primary visual cortex and the role of visual experience: dark rearing and monocular deprivation. *Vision Res.* **34,** 709–720 (1994).
3. Frenkel, M. Y. & Bear, M. F. How monocular deprivation shifts ocular dominance in visual cortex of young mice. *Neuron* **44,** 917–923 (2004).
4. Prusky, G. T., West, P. W. & Douglas, R. M. Experience-dependent plasticity of visual acuity in rats. *Eur. J. Neurosci.* **116,** 135–140 (2000).
5. White, L. E., Coppola, D. M. & Fitzpatrick, D. The contribution of sensory experience to the maturation of orientation selectivity in ferret visual cortex. *Nature* **411,** 1049–1052 (2001).
6. Antonini, A. & Stryker, M. P. Plasticity of geniculocortical afferents following brief or prolonged monocular occlusion in the cat. *J. Comp. Neurol.* **369,** 64–82 (1996).
7. Rittenhouse, C. D., Shouval, H. Z., Paradiso, M. A. & Bear, M. F. Monocular deprivation induces homosynaptic long-term depression in visual cortex. *Nature* **397,** 347–350 (1999).
8. Kirkwood, A., Rioult, M. C. & Bear, M. F. Experience-dependent modification of synaptic plasticity in visual cortex. *Nature* **381,** 526–528 (1996).
9. Duffy, F. H., Burchfield, J. L. & Conway, J. L. Bicuculline reversal of deprivation ambylopia in the cat. *Nature* **260,** 256–257 (1976).
10. Sillito, A. M., Kemp, J. A. & Blakemore, C. The role of GABAergic inhibition in the cortical effects of monocular deprivation. *Nature* **291,** 318–320 (1981).
11. Rauschecker, J. P. Cortical map plasticity in animals and humans. *Prog. Brain Res.* **138,** 73–88 (2002).
12. Barrett, B. T., Bradley, A. & McGraw, P. V. Understanding the neural basis of amblyopia. *Neuroscientist* **10,** 106–117 (2004).
13. Maffei, A., Nelson, S. B. & Turrigiano, G. G. Selective reconfiguration of layer 4 visual cortical circuitry by visual deprivation. *Nature Neurosci.* **7,** 1353–1359 (2004).
14. Egger, V., Feldmeyer, D. & Sakmann, B. Coincidence detection and changes of synaptic efficacy in spiny stellate neurons in rat barrel cortex. *Nature Neurosci.* **2,** 1098–1105 (1999).
15. Desai, N. S., Cudmore, R. H., Nelson, S. B. & Turrigiano, G. G. Critical periods for experience-dependent synaptic scaling in visual cortex. *Nature Neurosci.* **5,** 783–789 (2002).
16. Hensch, T. K. Critical period plasticity in local cortical circuits. *Nature Rev. Neurosci.* **6,** 877–888 (2005).
17. Thomson, A. M., Bannister, A. P., Mercer, A. & Morris, O. T. Target and temporal pattern selection at neocortical synapses. *Phil. Trans. R. Soc. Lond. B* **357,** 1781–1791 (2002).
18. Gaiarsa, J. L., Caillard, O. & Ben-Ari, Y. Long-term plasticity at GABAergic and glycinergic synapses: mechanisms and functional significance. *Trends Neurosci.* **25,** 564–570 (2002).
19. Woodin, M. A., Ganguly, K. & Poo, M. M. Coincident pre- and postsynaptic activity modifies GABAergic synapses by postsynaptic changes in Cl^- transporter activity. *Neuron* **39,** 807–820 (2003).
20. Holmgren, C. D. & Zilberter, Y. Coincident spiking activity induces long-term changes in inhibition of neocortical pyramidal cells. *J. Neurosci.* **21,** 8270–8277 (2001).
21. Simons, D. J. Response properties of vibrissa units in rat S1 somatosensory neocortex. *J. Neurophysiol.* **41,** 798–820 (1978).
22. Contreras, D. & Palmer, L. Response to contrast of electrophysiologically defined cell classes in primary visual cortex. *J. Neurosci.* **23,** 6936–6945 (2003).
23. Buzas, P., Eysel, U. T., Adorjan, P. & Kisvarday, Z. F. Axonal topography of cortical basket cells in relation to orientation, direction and ocular dominance maps. *J. Comp. Neurol.* **473,** 259–285 (2001).
24. Gibson, J. R., Bierlein, M. & Connors, B. W. A network of electrically coupled inhibitory neurons in neocortex. *Nature* **402,** 75–79 (1999).
25. Barlow, H. B. & Levick, W. R. The mechanism of directionally selective units in rabbits' retina. *J. Physiol.* **178,** 477–504 (1965).
26. Schoppa, N. E. & Urban, N. N. Dendritic processing within olfactory bulb circuits. *Trends Neurosci.* **26,** 501–506 (2003).
27. Kayser, A. S. & Miller, K. D. Opponent inhibition: a developmental model of layer 4 of the neocortical circuit. *Neuron* **33,** 131–142 (2002).
28. Hirsch, J. A. *et al.* Functionally distinct inhibitory neurons at the first stage of visual cortical processing. *Nature Neurosci.* **6,** 1300–1308 (2003).
29. Jin, X., Huguenard, J. R. & Prince, D. A. Impaired Cl^- extrusion in layer V pyramidal neurons of chronically injured epileptogenic neocortex. *J. Neurophysiol.* **93,** 2117–2126 (2005).
30. Kilman, V., van Rossum, M. C. & Turrigiano, G. G. Activity deprivation reduces miniature IPSC amplitude by decreasing the number of postsynaptic $GABA_A$ receptors clustered at neocortical synapses. *J. Neurosci.* **22,** 1328–1337 (2002).

Supplementary Information is linked to the online version of the paper at www.nature.com/nature.

Acknowledgements We thank R. Pavlyuk for help with histology, and A. Fontanini for help with software and for discussions. This study was supported by the National Institutes of Health.

Author Information Reprints and permissions information is available at www.nature.com/reprints. The authors declare no competing financial interests. Correspondence and requests for materials should be addressed to G.G.T. (turrigiano@brandeis.edu).